Catena 238 (2024) 107805

Contents lists available at ScienceDirect

Catena

journal homepage: www.elsevier.com/locate/catena

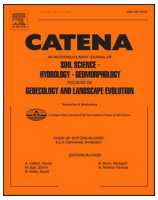

Effects of tropical cyclones on catchment sediment delivery to coastal ecosystems

Eliana Jorquera [a], Patricia M. Saco [a], Danielle Verdon-Kidd [b], José F. Rodríguez [a,*], Herman Timmermans [c], Filomena Nelson [d]

[a] School of Engineering and Centre for Water Security and Environmental Sustainability, The University of Newcastle, Callaghan 2308, Australia
[b] School of Environmental and Life Sciences and Centre for Water Security and Environmental Sustainability, The University of Newcastle, Callaghan 2308, Australia
[c] Pacific Community-SPC, Private Mail Bag, Suva, Fiji
[d] Secretariat of the Pacific Regional Environment Programme, PO Box 240, Apia, Samoa

A B S T R A C T

Coastal areas in the tropics are remarkably vulnerable to extreme weather-related events (e.g. floods, storm surge, erosion), which are expected to intensify in the future. Erosion of catchments is affected by changes in climate and vegetation, which alters the production of sediment transported into coastal areas and can lead to the loss of important ecosystem services. In many areas in the tropics, cyclones and depressions (TCs) produce the largest floods and massive discharges of sediment, which can affect coastal habitats in wetlands, lagoons and reefs. Here we focus on the Pacific Islands, but the methodology can be used in any tropical catchment affected by cyclones. A hydro-sedimentological model was used to analyse the sediment outputs of the Dreketi River (Fiji) and their relationship with cyclone activity over the last 45 years. The model was developed based on satellite and ground information on topography, soils, land use, and climatic data. The sediment export was related to TCs in the area, which were identified using the Southwest Pacific Enhanced Archive of Tropical Cyclones (SPEArTC) database. TC-related precipitation events were found to be three times more intense than non-TC events, and the average annual contribution of TCs to sediment export was about 25 %, with years contributing more than 50 %. TC-related events produced six times the sediment export of non-TC events, indicating a strong relation with precipitation intensity. Relations between precipitation rate and sediment export were developed for both TC and non-TC events, which can be used to predict the effects of increase of cyclone activity in the future.

1. Introduction

Coastal areas in the Pacific Islands are vulnerable to climate change in terms of sea level rise and extreme weather-related events (e.g. floods, storm surge, erosion), all of which have seen a continuous increase over the past years (Saco et al., 2021). According to several studies, one of the most destructive natural hazards in the tropical South Pacific are tropical cyclones and tropical depressions (TCs) (Lafale et al., 2018, Magee et al., 2016b, McInnes et al., 2014, Terry and Gienko, 2010) both in terms of number of people affected and monetary losses due to the resulting damages. The yearly average economic impact of tropical cyclones can count up to six percent of the Gross Domestic Product (GDP) per year, affecting the infrastructure, agriculture and buildings (World Bank Group, 2017). The scale of impact is due to a combination of two factors: the low-lying nature/high vulnerability of the Pacific Islands Countries (PICs) and the severity of the events. Among the PICs, the Republic of Fiji is the second largest and most populated (Barnes, 2020). It has been listed in the top 20 most hazardous countries in the world by WorldRiskIndex during the past ten years (Behlert et al., 2020). According to the Government of Fiji (2017) during the last decades (1970 – 2016) a cumulative number of almost 1.9 million people have been affected by at least one TC.

One of the primary impacts of TCs is flooding. A study by Kostaschuk et al. (2001) showed that for the Fiji Islands, more floods are caused by tropical rainstorms than by TCs, but TC floods tend to be larger. TC-related floods also produce significant amounts of sediments that end up in wetlands, coastal lagoons, and reefs, potentially endangering important coastal ecosystems (Brown et al., 2017). Sediment supply to coastal wetlands and shorelines is also of critical importance for accretion processes that enable them to cope with sea-level rise (Rodriguez et al., 2017, Sandi et al., 2018, Breda et al., 2021). However, long term measurements of sediment loads into Fiji's coastal areas are not available (a common issue across most of the Pacific Islands). To address this constraint, hydro-sedimentological models can help quantify sediment yield of the catchments upstream to coastal ecosystems (Pandey et al., 2016). Furthermore, calibrated models are a very useful tools to assess

* Corresponding author.
E-mail address: jose.rodriguez@newcastle.edu.au (J.F. Rodríguez).

https://doi.org/10.1016/j.catena.2024.107805
Received 16 August 2023; Received in revised form 3 November 2023; Accepted 3 January 2024
Available online 30 January 2024

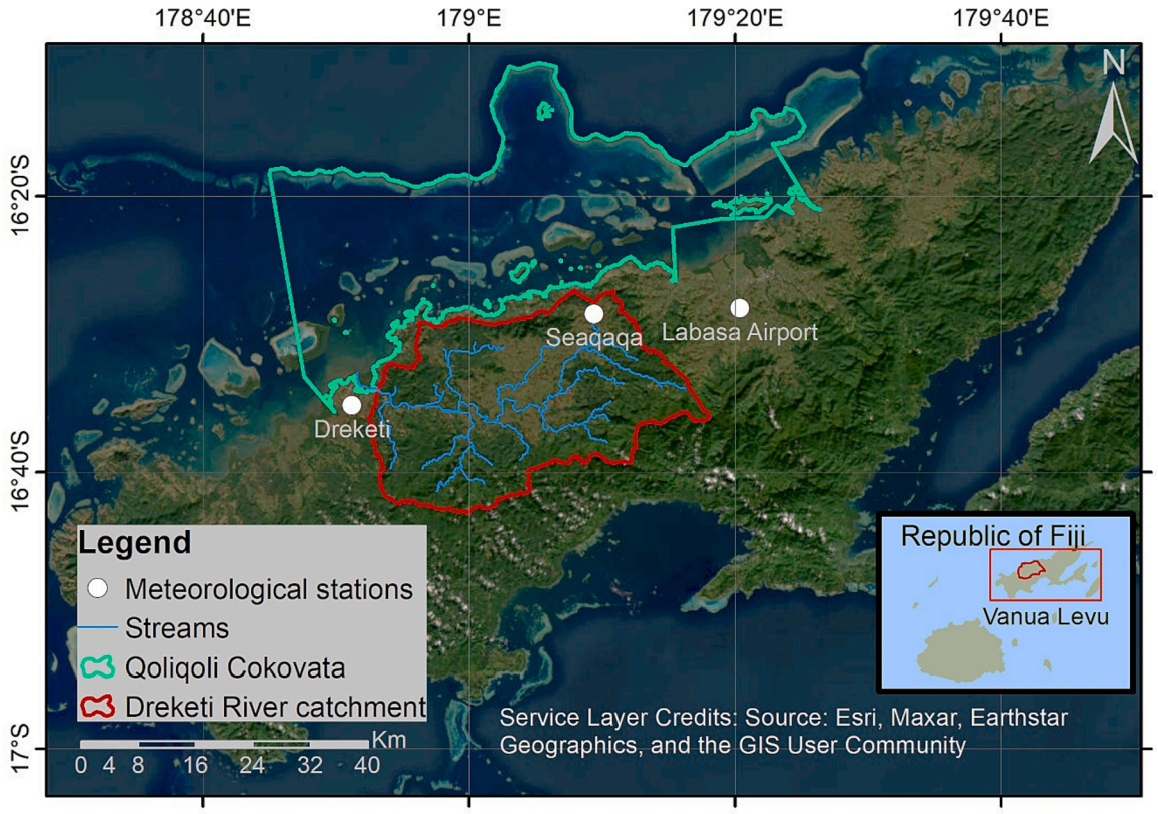

Fig. 1. Geographic location of Qoliqoli Cokovata, Dreketi River catchment and its meteorological stations.

the behaviour of the area under future climate scenarios.

Despite recent advances, soil erosion and sediment yield at the catchment scale remains a challenging topic due to the complex interactions between land cover, land use, and climate (de Vente et al., 2013, Quijano-Baron et al., 2022). In addition, the availability of reliable data is often limited, making it difficult to accurately model soil erosion and sediment yield. The range of strategies to quantify erosion and sediment transport can be grouped into field measurements, empirical-statistical models, and physically-based soil erosion–deposition models (Wu et al., 2012, Chiu et al., 2019). Although field measurements could potentially provide the most accurate results, most regions (and in particular the Pacific Islands) lack long-term records of sediment variables. Empirical models are mainly derived from the Universal Soil Loss Equation (USLE), Modified Universal Soil Loss Equation (MUSLE) and Revised Universal Soil Loss Equation (RUSLE) (Hudson, 1993, Smith and Wischmeier, 1957, Wischmeier et al., 1958, Wischmeier, 1959, Williams and Berndt, 1977). Some of these models need to be applied jointly with Sediment Delivery Ratio (SDR) to calculate the sediment export, which has a high level of uncertainty in its determination (de Vente et al., 2013). Physically-based models represent an improvement over the estimations of the empirical models (Chiu et al., 2019). They use the conservation of mass, momentum, and energy for the water flow, combined with an empirical formulation for the sediment yield and transport (Wu et al., 2012). For instance, the Agricultural Non-Point Source Pollution Model AGNPS (Bingner and Theurer, 2016, Bingner and Theurer, 2001) and the Open-Source Version of the Nonpoint Source Pollution and Erosion Comparison Tool, OpenNSPECT, (Eslinger et al., 2014), use the USLE equation, while SedNET (Sediment River Network Model) (Wilkinson et al., 2009), WaTEM-SEDEM, Water and Tillage Erosion Model/ Sediment Delivery Model (Notebaert et al., 2006) and the Integrated Valuation of Ecosystem Services and Tradeoffs InVEST (Sharp et al., 2018) apply the RUSLE method. Other models, like the Soil and Water Assessment Tool, SWAT, (Arnold et al., 1998) and CREAMS (Chemicals/Runoff, and Erosion from Agricultural Management Systems) (Knisel and Douglas-Mankin, 2012, Knisel, 1980) implement the MUSLE procedure. In addition to estimating the processes of production and transport of sediments, most of these models also compute the production and transport of pollutants. The advantage of the physically-based models over the other methods is their ability to capture additional geographic and hydrological factors in the catchment (Pandey et al., 2016). Several studies have compared the performance of the different available models under a wide range of conditions (Merritt et al., 2003, Vigerstol and Aukema, 2011, Alvarez-Romero et al., 2014, Liu et al., 2017, Abdelwahab et al., 2018, Nguyen et al., 2019, Pandey et al., 2016). The general agreement is that the selection of the most suitable model will depend on the particular questions and problems that are being addressed (Hajigholizadeh et al., 2018). In other words, beyond the general characteristics of each soil erosion and sediment yield model, it is necessary to consider how the specific objectives of the study and the data availability reflect the conditions of the catchment. In this paper, the SWAT model was selected to simulate the hydro-sedimentological behaviour of the catchment due to model requirements and data availability.

The aim of this work was to characterise the hydro-sedimentological behaviour of the catchment, assess the impact of TCs on the annual sediment budget, and explore the relationship between precipitation and sediment export for TC-related and TC-unrelated precipitation events. After calibration and validation using remote sensing information on suspended sediment the SWAT model was run from 1970 to 2017 (with a daily time step) and events related to TCs were identified using the SPEArTC database.

2. Materials and methods

Among the Pacific Islands Nations, the Republic of Fiji is well known for the rich biodiversity of its coastal areas. It has more than 300 islands and 500 islets distributed over more than 1.3 million square kilometres of the South Pacific (Mangubhai et al., 2019). However, 80 % of its land

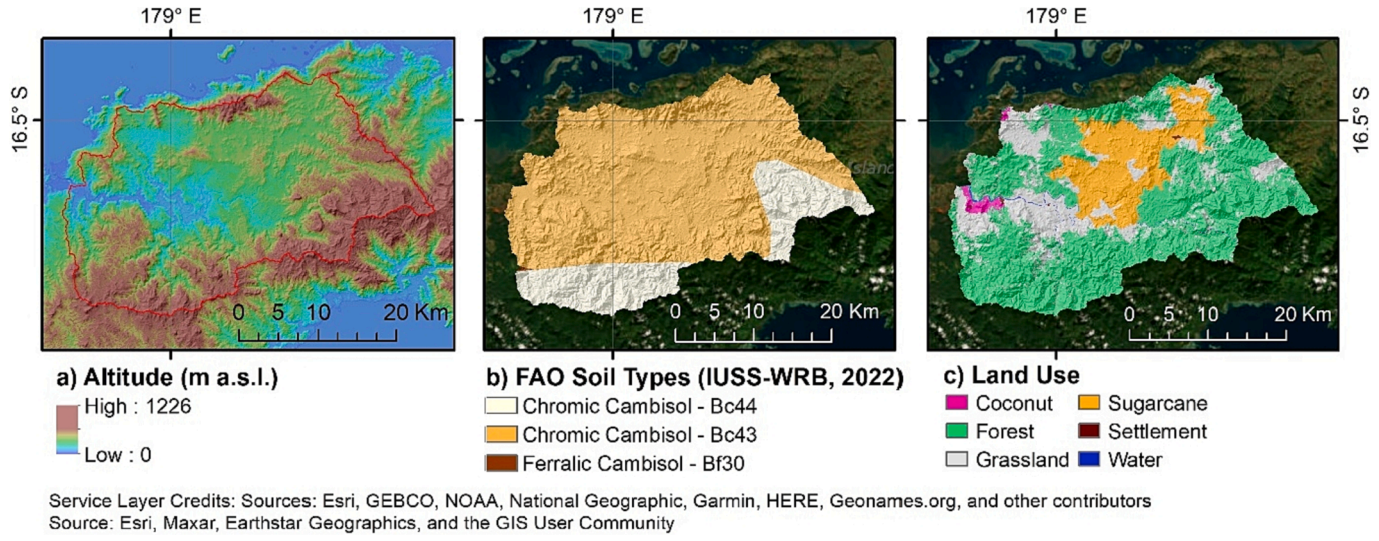

Fig. 2. Spatial maps of the Dreketi catchment. a) Digital Elevation Model (SRTM), b) FAO Soil Taxonomy Map (Adapted from World Reference Base for Soil Resources digital soil map of the world (IUSS-WRB, 2022)), c) Land Use/Land Cover Map (Adapted from (PCRAFI, 2010)).

Table 1
Available meteorological data.

Station	Location			Available periods				
	Latitude	Longitude	Elevation	Precipitation	Maximum and minimum air temperature	Sunshine duration	Wind Speed	Relative Humidity
Dreketi	16°35′11″ S	178°51′12″E	4	1/1/1977 – 31/12/2017	1/1/1977 – 31/12/2017		1/7/1982 – 31/12/2017	1/2/1982 – 31/12/2017
	Missing data			3.3 %	19.5 % Tmax – 21.7 % Tmin			15.5 %
Seaqaqa	16°28′33″S	179°9′28″E	101	1/1/1970 – 31/12/2017	6/9/1972 – 31/12/2017	1/7/1971 – 31/12/2017	1/1/1973 – 31/12/2017	6/9/1972 – 31/12/2017
	Missing data			2.8 %	7.8 % Tmax – 9.6 % Tmin			5.1 %
Labasa Airport	16°28′8″S	179°20′23″E	13	1/1/1970 – 31/12/2017	1/1/1970 – 31/12/2017	–	1/1/1970 – 31/12/2017	1/1/1970 – 31/12/2017
	Missing data			2.4 %	2.7 % Tmax – 6.3 % Tmin	6.3 %		4.5 %

and 90 % of the population are concentrated on the two main islands of Viti Levu and Vanua Levu (Agrawala et al., 2003); with Vanua Levu being the less populated with only 15 % of the population. Along the northern coast of Vanua Levu is the Great Sea Reef, known locally as Cakaulevu, which extends for 260 km and is the third longest continuous barrier reef system in the world (SPREP, 2017).

In 2018 the central area of the Cakaulevu was designated as a Ramsar Site (No. 2331), Qoliqoli Cokovata (Ramsar Convention Secretariat, 2019). Among the catchments draining to the Qoliqoli, the Dreketi River catchment is one of the main sediment contributors (Brown et al., 2017) and it has an extensive mangrove wetland at the mouth of the river (Fig. 1). With an area of 825 km^2, the catchment has a rugged topography at its headwaters with slopes greater than 30 %, mainly in the southern area of the catchment. The northern and central area of the catchment has smoother topography. The main river (Dreketi) has a total length of 73 km. The confluence of the Nanenivuda and Korovuli rivers gives origin to the Dreketi River, and downstream its major tributaries are the Nasuva, Seaqaqa, Vumbelebele and Naua rivers (Jorquera et al., 2019). The area has a tropical marine climate, there is a strong wet season from November to April with an average monthly precipitation of 300 mm per month, and much of this precipitation is generated by tropical depressions that can intensify to tropical cyclones. During the dry season, the average monthly precipitation is 80 mm. The variations in temperature are small, with a decrease of the average maximum and minimum temperature of one and four degrees respectively, during the coldest months (June to August) (FMS, 2006).

2.1. Topography, soil **types** and land cover data

A Digital Elevation Model (DEM) derived from the Advanced Spaceborne Thermal Emission and Reflection Radiometer of Global DEM (ASTER GDEM) (https://lpdaac.usgs.gov) was used for the Dreketi River catchment. The spatial resolution is one arc-second (30 x 30 m) (Fig. 2a).

Soil type coverage (Fig. 2b) was based on a digital layer from the Food and Agriculture Organization (FAO) of the United Nations (UN) and the UN Educational, Scientific and Cultural Organization (UNESCO) published and updated since 1981 (Sanchez et al., 2009). This digital layer is low resolution (250 x 250 m pixels), but the information related to each soil Mapping Unit was useful to determine soil properties like texture, slope classes, depth of profile, and composition among other characteristics. Furthermore, the classification was compatible with the SWAT database for soil properties, which is based on the FAO/UNESCO soil types. The dominant soil in the catchment is the Chromic Cambisols, which has uniform medium-textured profiles, with organic surface horizons overlying reddish or brownish subsoils. It is a moderate well drained soil with a high clay content (IUSS-WRB, 2022).

The land use layer (Fig. 2c) was obtained from the Pacific Catastrophe Risk Assessment and Financing Initiative (PCRAFI) – Pacific Risk Information System - OpenDRI repository for the Pacific Region (https://pcrafi.spc.int/). The land use map indicates that 80 % of the catchment is covered by forest and grassland. The remaining 20 % is distributed among different crops, surface waters, low-density urban settlements, forestry and gravel extraction. The dominant crop is

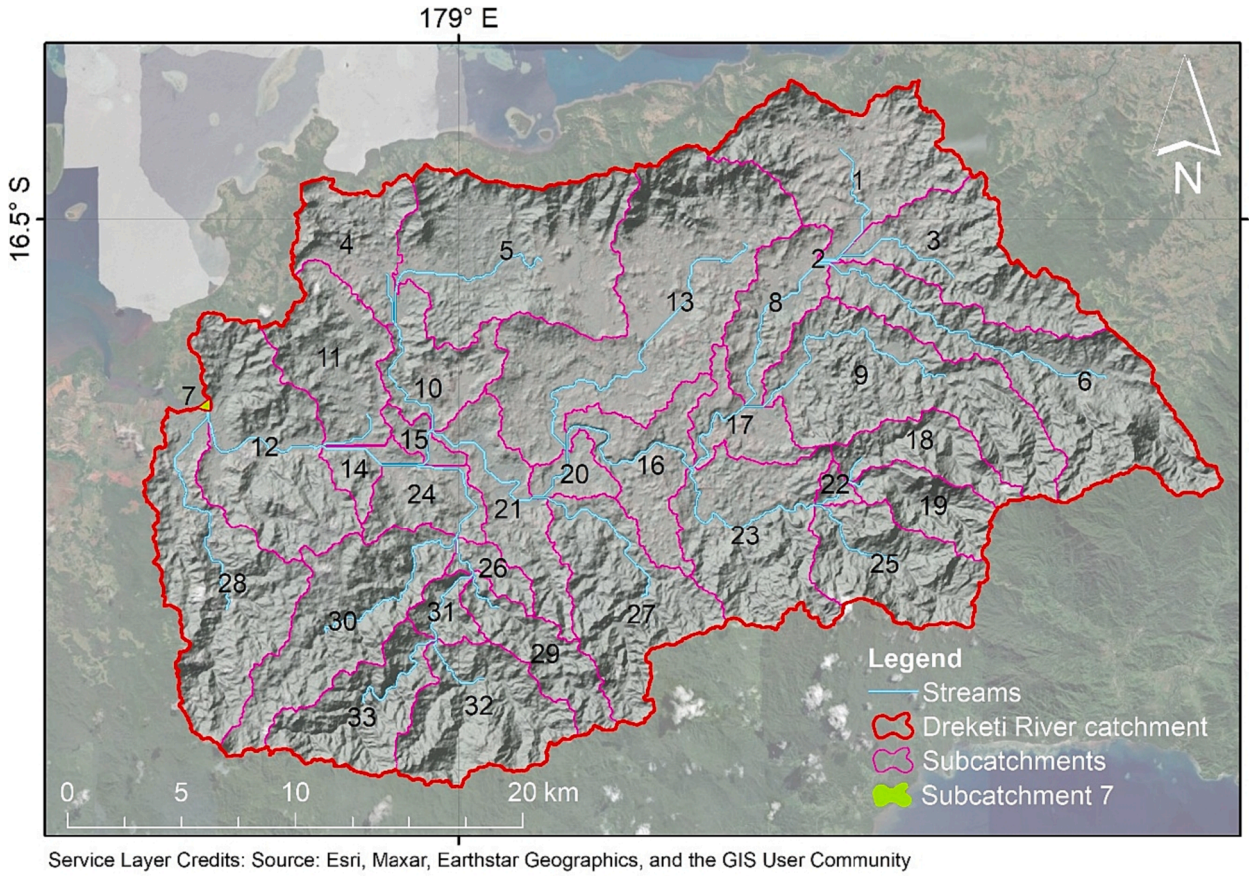

Fig. 3. SWAT spatial discretisation, 33 subcatchments.

sugarcane, with a small percentage of coconut. Other minor crops are: rice near the mouth of the Dreketi River and taro, cassava and kava in the villages (PCRAFI, 2010).

2.2. Meteorological *data*

The meteorological data required for the hydrological modelling included daily precipitation, temperature, relative humidity, wind speed and solar radiation. All the information processed is from the Fiji Meteorological Service (FMS). For the Dreketi River basin, there are three stations nearby, Dreketi, Seaqaqa and Labasa Airport (Fig. 1). For precipitation data the record period is from 01/01/1970 to 31/12/2017 for Seaqaqa and Labasa Airport stations while for Dreketi station is from 01/01/1977 to 31/12/2017. All three have precipitation, maximum and minimum air temperature, wind speed and relative humidity daily data. The sunshine duration daily is only available from the Seaqaqa station. Table 1 summarises the available data for the catchment.

SWAT runs on daily meteorological data but accepts lower temporal resolution data that is disaggregated using an onboard weather generator. The criterion for data selection was that the amount of missing daily data was small enough to apply a gap-filling procedure based on correlation between stations. When the data could not meet the criterion, the monthly data was used jointly with the weather generator. Based on these analyses and the quality of our data (Table 1), the decision was to work with daily data for precipitation, temperature and relative humidity; and monthly for wind speed and solar radiation. Solar radiation was estimated using the Angström-Prescott method that relates solar radiation with sunshine duration, the day of the year, latitude and longitude (Iqbal, 1983).

Another important meteorological data required by SWAT is the monthly maximum 30-min precipitation. This value is used to calculate the time of concentration in each sub-catchment, which will affect the peak discharge and thus the sediment yield (Neitsch et al., 2011, Yáñez-Arancibia et al., 2011). When only daily data is available, a peak intensity coefficient, i.e. the ratio of monthly maximum 30-min precipitation to monthly maximum daily precipitation can be used (García et al., 2001, Tucci, 2012). However, this peak coefficient varies monthly and can also vary for different climatic regions in the world. Therefore, to determine a local estimate of the peak coefficient data from a high temporal resolution meteorological station located in American Samoa that has a similar climate to Fiji (see supplementary material) was used.

2.3. Hydro-sedimentological model

The inputs for SWAT include topography, soil type, land use and climate data. The first three, are used to discretize the catchment spatially into sub-basins and hydrologic response units (HRUs) (Neitsch et al., 2011). The density of the stream network and the number of sub-basins are based on the DEM and a threshold drainage area. The definition of HRUs, depends on the soil, land use and slope classes map. Furthermore, runoff, infiltration and erosion processes will depend on the DEM, soil type and land cover; for instance, the hydrology module and the USLE methodology described later requires curve number value CN, Manning's coefficient n, soil erodibility factor K, crop management factor C, and slope-lenght factor SL.

The climate data drives the hydrological processes in the catchment. The standard data needed are precipitation, temperature, relative humidity, wind speed and solar radiation. The hydrological balance equation is solved in each HRU, estimating the amount of water that will reach the channel network (Arnold et al., 1998). The balance equation expressed in mm is:

Table 2
Slope classes (following Atherton et al., 2005).

Slope Classes	Slope		Erosion risk
	Percentage	Degree	
1	0 – 3.5	0 – 2	Very low
2	3.5 – 30	2 – 16	Low
3	30 – 50	16 – 26	Moderate
4	50 – 60	26 – 31	Steep
5	Over 60	Over 31	Extreme

$$SW_t = SW_0 + \sum_{i=1}^{t} (R_i - Q_{surf_i} - ET_i - w_{seep_i} - Q_{gw_i}) \quad (1)$$

where SW_t is the soil water content at day t, SW_0 is the initial soil water content. All the variables with the subscript i referred to the day i, being R the precipitation, Q_{surf} surface runoff, ET actual evapotranspiration, w_{seep} flow entering the vadose zone and Q_{gw} the return flow or groundwater flow.

The surface runoff is routed through the channel network, and the sediments, nutrients and pollutants are transported by this surface runoff. The sediment yield is obtained from the MUSLE equation (Williams and Berndt, 1977) applied to each HRU.

$$y = 11.8 \cdot (Q \cdot q_p \cdot A_{HRU})^{0.56} K \cdot C \cdot SL \cdot P \cdot CFRG \quad (2)$$

where: y is the sediment yield (tonnes), Q runoff volume (m^3) and q_p the Peak runoff rate (m^3/s). K, C, SL and P are the standard USLE factors for soil erodibility, crop management, slope length-gradient and erosion control practice, respectively. A_{HRU} represents the area of the HRU and CFRG the coarse fragment factor.

SWAT has on-board pre-defined databases that relate land use and soil types with hydrological, erosion and plant grow parameters, among others. The user can match those with their data or can add known parameters.

Based on the DEM we varied the threshold area of flow accumulation to obtain a spatial resolution in the catchment that would result in a stream network that resembles the observed stream network identifiable with satellite information. A threshold area of 1250 ha for flow accumulation resulted in 33 sub-catchments (Fig. 3) and a stream network closely representing the observed network. The HRU were classified based on soil types, land uses and slope classes. The slope classes were defined based on thresholds suggested for erosion risk in the area (see Table 2, Atherton et al., 2005).

The model was run from 1970 to 2017 with a daily time step. The first two years were used as a warm-up. The model was calibrated using the sediment concentration at the outlet of the catchment. We also carried out additional model verification using limited hydraulic information as explained in more detail in the results section.

SWAT has parameters that affect the sediment yield indirectly or directly. Among the first group are those related with the surface runoff. In the second group are the explicit parameters of the sediment production and transport. Table 3 presents some of the main parameters in both categories. In the calibration process of the first group the channel and overland roughness coefficients (Manning's n) were modified. SWAT default values are 0.014 for both channel and overland flow. A value of 0.035 was adopted for the channel and the overland varies between 0.14 and 0.8 according to the land use (Table 3). The Curve Numbers (CN2) are estimated within SWAT as a function of the soil type, and they were not changed.

Two main processes are represented in the sediment module of SWAT. First, the landscape component calculates the amount of sediment that each sub-catchment can produce according to the MUSLE equation applied to each HRU (equation (2). Most of the parameters of equation (2) have a physical meaning, like the flux (Qq_p), soil type (K), topography (SL) or the land use (C). The parameter P depends on the management practice. In this case a unit value for P was adopted for the agriculture land use, and 0.5 for the naturals areas (forest and grassland) following Li et al. (2014) and Benavidez et al. (2018). All the other parameters remained with the default value that corresponded with the soil type, land use or topography.

Not all the sediment produced at the HRUs (equation (2) will reach the streams. Sediment is transported via overland flow and can be trapped by vegetation and local topographic features (ponds). The remaining sediment is added to the incoming sediment contribution that enters the stream. The dominant process on the channel, deposition, or degradation, is calculated comparing the incoming concentration of sediment that reaches the channel (potentially from more than one HRU) with the transport capacity of the reach. The transport capacity is calculated according to a simplified version of the Bagnold stream power equation, in which the transport capacity from a reach segment is a function of the peak channel velocity.

$$conc_{sed,ch,mx} = c_{sp} \cdot v_{ch,pk}^{spexp} \quad (3)$$

where $v_{ch,pk}$ is the peak channel velocity (calculated using Manning's

Table 4
Performance indicators for daily values.

Subbasin	7	12	15
NSE	0.83	0.68	0.80
PBIAS	14 %	13 %	−7%
RSR	0.41	0.57	0.45

Table 3
SWAT parameters.

Surface	Parameter	Description	Range	Influencing factor	References	Adopted value
Runoff	CN2	Curve number at moisture condition II	30–98	land use, soil and slope	(Neitsch et al., 2011)	
	CH_N2	Channel Manning's roughness coefficient	0–0.67	(calibrated) channel bed and banks characteristics	(Briak et al., 2016, Vilaysane et al., 2015)	0.035
	OV_N	Manning's roughness coefficient for overland flow	0.1–12	(calibrated) land use and vegetative cover	(Ricci et al., 2018)	Agriculture: 0.14; Grassland: 0.6; Forest:: 0.8
Sediment Processes	USLE_K	Soil erodibility factor	–	soil type	(Benavidez et al., 2018, Neitsch et al., 2011)	
	USLE_C	Cover and management factor	0.001 – 0.5	land use	(Benavidez et al., 2018, Neitsch et al., 2011)	
	USLE_SL	Topography factor	–	topography, from the DEM	–	
	USLE_P	Support practice factor	0–1	management practice	(Benavidez et al., 2018, Li et al., 2014)	Natural areas. 0.5; Agriculture. 1
	SPEXP	Exponent in sediment transport equation (Bagnold equation)	1 – 1.5	(calibrated)	(Neitsch et al., 2011)	1.5
	SPCON	Coefficient in sediment transport equation c_{sp}	0.0001–0.001	–	(Neitsch et al., 2011)	0.0001

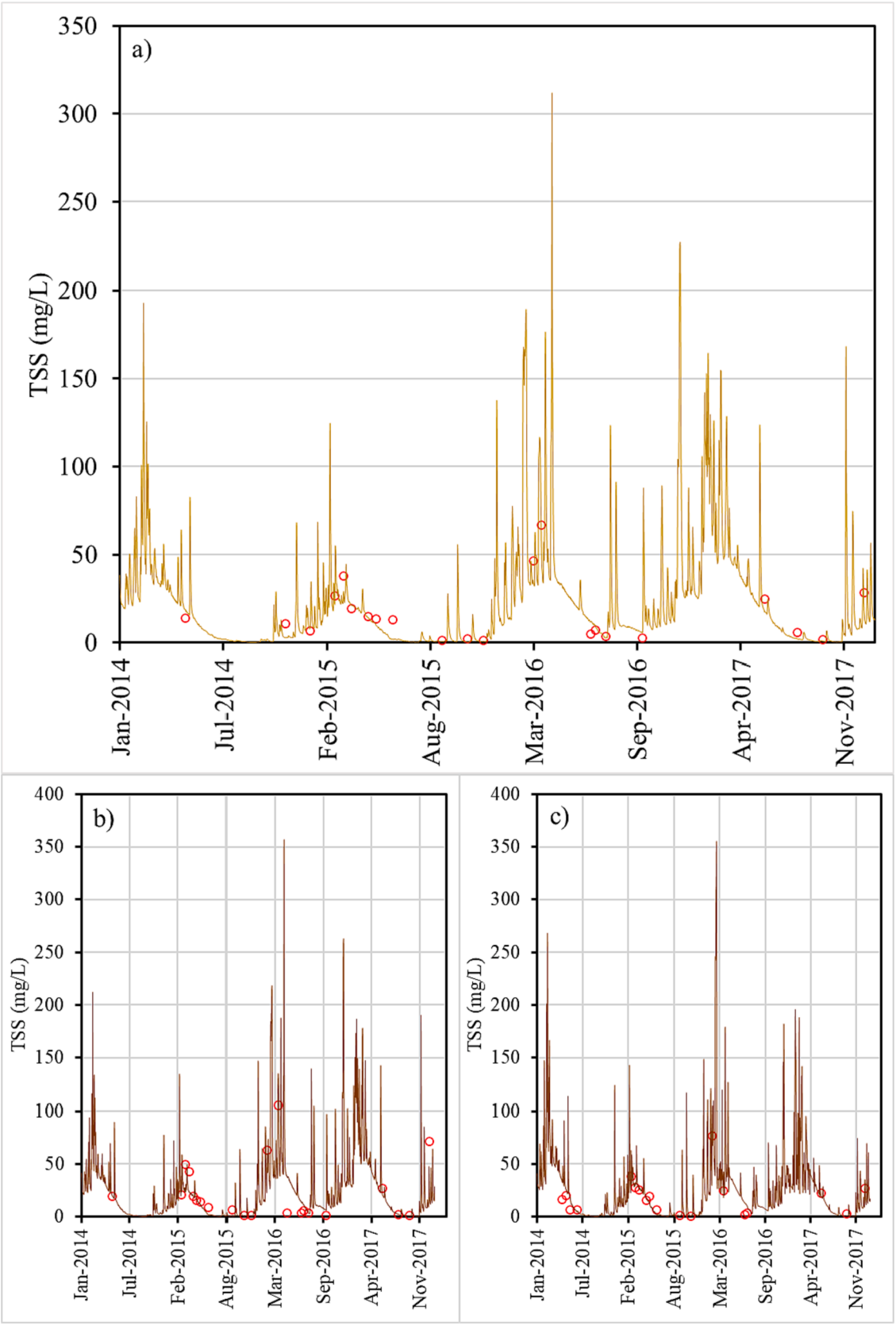

Fig. 4. a) Sedimentograph at the outlet of the catchment (subcatchment 7). Sedimentograph at sub-catchments 12 (b) and 15 (c). Solid line represents TSS from SWAT simulation and dots from C2RCC.

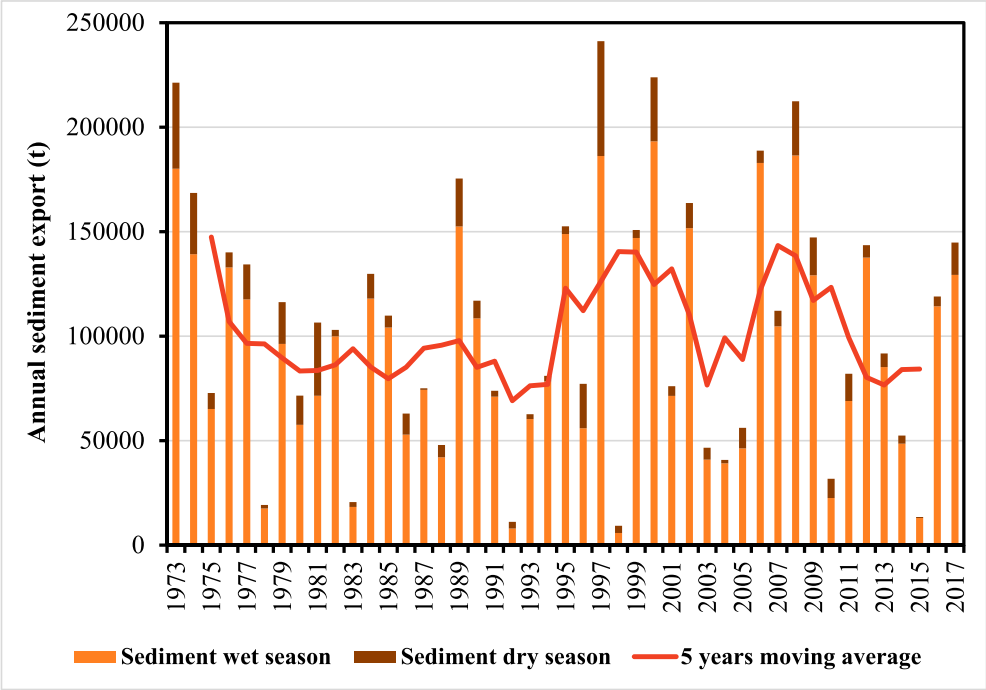

Fig. 5. Sediment yield per hydrological year at the outlet of the catchment. The line indicates the five years moving average.

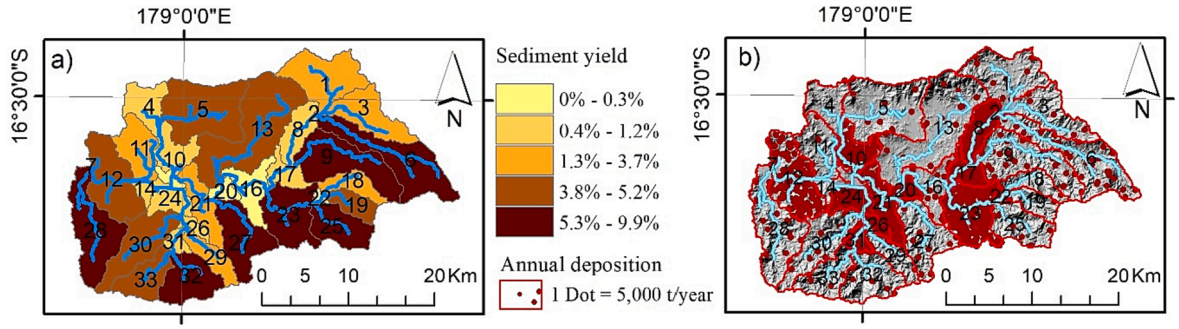

Fig. 6. a) Relative contribution per sub-catchment of the total sediment yield. b) Average annual sediment deposition per sub-catchment.

equation and the peak intensity coefficient) and c_{sp} and spexp are user-defined coefficients. The coefficient spexp varies between 1.0 and 1.5 and was adjusted during the calibration process, and c_{sp} varies between 0.0001 and 0.001. The transport capacity of the stream ($conc_{sed,ch,mx}$) is compared with the incoming sediment concentration. Deposition occurs if the incoming sediment concentration is higher than the transport capacity, and erosion occurs if it is lower.

Once the model was calibrated, an analysis of the spatial and temporal distribution of the sediment yield was performed. To analyse the temporal pattern of the sediment yield we defined the hydrological year from July to June to have the entire cyclone season (November to April) within the year. The year was named using the last year, for instance the hydrological year from July 1972 to June 1973 was named as 1973, to follow the convention used in the TCs data.

The spatial distribution of the sediment over the entire hydrological year and during the wet and dry season was studied, first at sub-catchment level and then at HRU (Hydrologic Response Unit) level.

2.4. Remote sensing data for total suspended solids (TSS)

Satellite data was used to calibrate the sediment outputs of the hydro-sedimentological model. The images retrieved from Landsat 8 and Sentinel-2 were first selected according to the cloudiness cover over the area of interest, setting a limit threshold of 10 %. A total of 83 Landsat and 60 Sentinel-2 images were retrieved from 2013 to 2018. Then, the Case-2 Regional Coast Colour (C2RCC) processor (Brockmann et al., 2016) available on the European Space Agency's (ESA) Sentinel toolbox SNAP was applied (https://step.esa.int/). The C2RCC is based on the Case 2 Regional processor, originally developed by Doerffer and Schiller (2007). It estimates the inherent optical properties (IOPs), such as absorption and scattering coefficients from the water, leaving radiance reflectance measured at the top of the atmosphere. Those values are used to calculate the concentrations of optically active substances such as total suspended matter and chlorophyll *a*. It is a multi-mission ocean colour processor composed of a set of neural networks trained with a large dataset (approximately 5 million cases) to transform the top-of-atmosphere radiances into IOPs and finally convert them into the concentrations mentioned. It has been trained to cover extreme ranges of scattering and absorption and performs two quality checks to verify that the reflectance is within the training range. C2RCC has been validated in various studies for the different sensors with good results for case 2 water (Brockmann et al., 2016, Nazirova et al., 2021, Breda et al., 2022).

The calibration was carried out at the outlet of the catchment, sub-catchment 7, and validated in two additional sections upstream, sub-catchments 12 and 15 (Fig. 3 and Fig. S.3 from supplementary information). Those sections were selected because the stream was wide

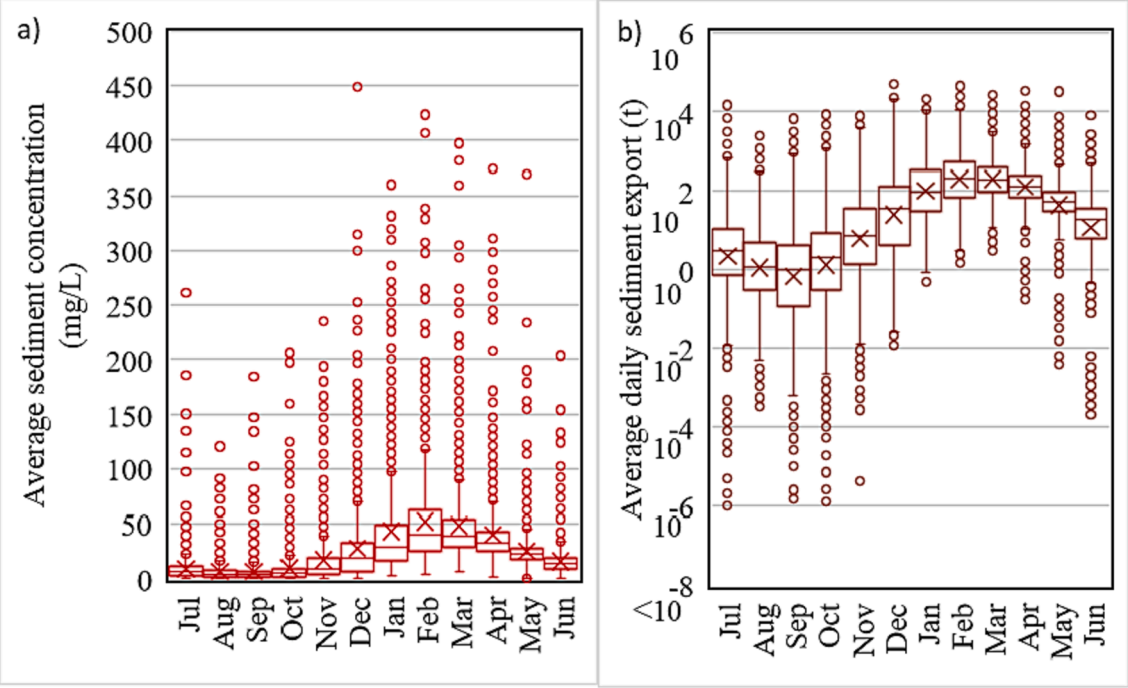

Fig. 7. a) Average daily sediment concentration and b) average daily sediment export at the catchment outlet (sub-catchment 7).

enough (50 to 120 m) so that a reliable estimate of the suspended solids could be obtained from the satellite information. Further inland, the size of the streams did not allow for a clear identification of suspended solids (Fig. S.3). The catchment outlet was defined at the outlet of sub-catchment 7 as this location was the most downstream point of the catchment that was not affected by the tidal effect.

2.5. Tropical cyclones and depressions data

There are several databases of the regional tropical cyclone information for the Southern Hemisphere. The Southwest Pacific Enhanced Archive of Tropical Cyclones, SPEArTC (Diamond et al., 2012), has been acknowledged as the most complete repository for this area (Sharma et al., 2020, Magee et al., 2016a). The database contains the coordinates and central pressures for each cyclone and tropical depression throughout its life, at mostly 6-hourly intervals, for tropical cyclones (TCs) since 1840 (noting that TC data post the mid 1940 s is more reliable/complete and the earlier data must be used with caution).

To assess the impact of TCs on flood derived sediment loads to the Dreketi River catchment, cyclones were considered to potentially affect the catchment if their tracks were located within 550 km of the centre of the catchment (17°S, 178.5°E) and within a time window of ± 1 day (Fig. 8). This approach has been followed by several authors relating the impact of TCs on extreme precipitation events (Khouakhi et al., 2017, Deo et al., 2021, Villarini and Denniston, 2016, Dare et al., 2012). The analysis period was from 1970 to 2017, but the first two years were not considered (warm-up period for the hydro-sedimentological modelling).

Using the calibrated model, the impact of TCs was assessed. Precipitation events were cross matched to TCs to identify TC related precipitation events based on the information obtained from the SPEArTC database. A precipitation event was defined as a series of consecutive days of accumulated precipitation until a day with no precipitation. If during the days of the event it was possible to identify a TC within the area, the event was classified as a TC related event. Then, the sediment yield from those events was assigned to the corresponding TC.

3. Results

3.1. Model calibration

The suspended sediment concentrations were retrieved from analysis of satellite information for several events at the outlet of the catchment (sub-catchment 7) and at two other locations further inland. The performance of the model was assessed comparing those measured values with the model results following the guidelines given by Moriasi et al. (2007). The three quantitative statistics used were: the Nash–Sutcliffe efficiency (NSE), percent bias (PBIAS) and ratio of the root mean square error to the standard deviation of measured data (RSR). Moriasi et al. (2007) suggested that, for monthly values, the general performance rating is very good if RSR is between 0 and 0.50, a NSE is greater than 0.75 and an absolute value of PBIAS is less than 15 %. There are no suggested values of performance indicators for daily values, but the common practice is to accept larger errors for shorter time steps. The best values of the performance indicators obtained after calibration (sub-catchment 7) and validation (sub-catchments 12 and 15) (see Fig. 3) are presented in Table 4. Calibration was very good considering that the data was daily, with RSR = 0.41, NSE = 0.83 and PBIAS = 14 % (Fig. 4a). Performance deteriorated for the validation sub-catchments but was still acceptable (Fig. 4b and c).

Model results from Fig. 4 shows that the sediment values in internal sub-catchments (12 and 15) are higher than at the catchment outlet (7) indicating deposition within the catchment. Even with this internal deposition, the sediment exiting the catchment is considerable..

The bankfull discharge concept was used as an additional way of verifying the performance of the model. The bankfull discharge can be defined according to the morphology of the cross-section or with a statistical analysis of the flows. In terms of the recurrence interval, the bankfull discharge is defined as the discharge that overtops the banks every year or every other year, with a median value of about 1.5 years (Wolman and Leopold, 1957, Gordon et al., 2004). Considering the channel morphology, Harrelson and Rawlins (1994) provided a guide to identify the bankfull stage and the boundaries of the active floodplain, and once the bankfull cross-section has been identified the discharge can be calculated using the Manning equation (Fernandez, 2017).

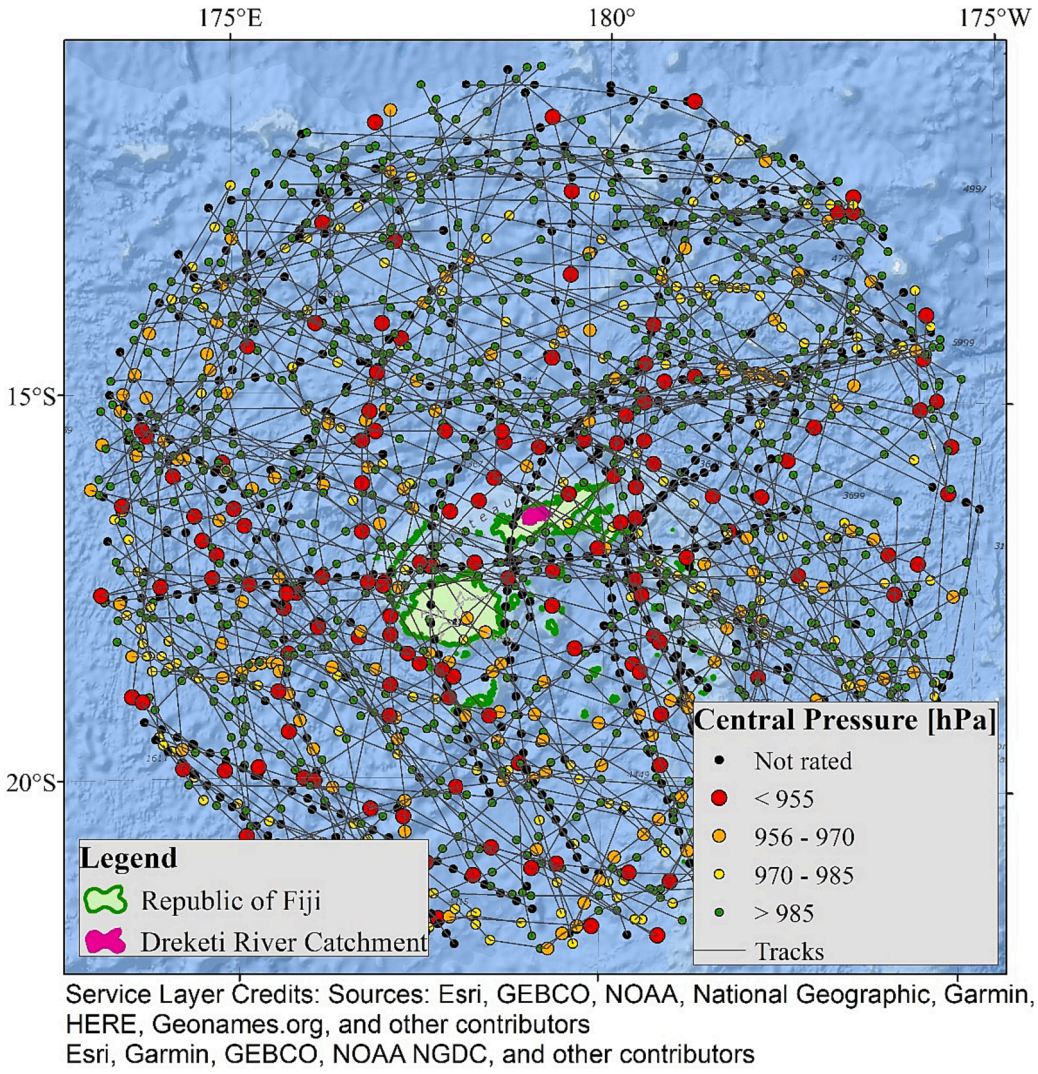

Fig. 8. Cyclones from the SPEArTC from 1970 to 2018 within a radius of 5° from the centre of the catchment.

For the Dreketi River, there is a well-documented section in the eastern headwaters of the catchment, the Dreketi River cross-section at Natua village (Terry et al., 2004). Following Harrelson and Rawlins (1994) the bankfull section was identified (see supplementary information Fig. S.4 and Fig. S.5), and the main characteristics are: width 32.7 m, area 52.8 m^2, wetted perimeter 34.0 m and slope 0.0021 m/m. Applying the Manning equation with a roughness coefficient of 0.035 we have a discharge of 92 m^3/s. To validate our simulation, the discharge calculated with the Manning equation was compared with the simulated discharge with a recurrence of 1.5 years. Adjusting a Log-Pearson III distribution to the maximum annual flows, the one in 1.5 years discharge was equal to 88 m^3/s.

3.2. Sedimentological behaviour of the catchment: spatial and temporal analysis of sediment export

The sediment export at the outlet of the catchment for each hydrological year is shown in Fig. 5. The average sediment export was around 120,000 Tn/year but varied considerably from 10,000 to 240,000 Tn/year. The two different colours represent the sediment export in the wet, or cyclone season (orange) and the contribution of the dry season to the total annual sediment export (brown). For the period analysed, on average, 79 % of the precipitation fell during the wet season producing 87 % of the annual sediment export. The wet season with the lower contribution, 63 % for precipitation and 65 % for sediment, was during the 1997–1998 season (named 1998 in the figure) due to the drought caused by an El Niño event (Terry and Raj, 1999a). The higher relative contribution was during 1986 – 1987, mainly due to cyclone RAJA, while the sediment export during the wet season in 1999–2000 was the absolute maximum for the period analysed, almost doubling the average value. However, the maximum sediment export for an entire year was registered in 1996 – 1997, due to cyclone JUNE that affected Fiji during early May which in this analysis was part of the dry season.

Fig. 6a shows the relative contribution of each sub-catchment to the total sediment yield However, sediment export at the catchment outlet (sub-catchment 7) is significantly lower, which is a response to the topographic characteristics of the catchment. Fig. 6b presents the average annual deposition per sub-catchment. The river's average slopes in the headwater, the mid reach, and the lower plain are 0.8, 0.4 and, 0.2 percent, respectively (Fig. S.6), while the average slope of the headwater, mid reach, and lower plain sub-catchments are 22.0, 15.0 and 11.6 percent, respectively. Those slope differences can explain the sediment deposition observed in the lower plain.

Regarding the sediment concentration at the catchment outlet, Fig. 7a shows the average daily TSS grouped by month. It can be seen that the average monthly TSS is three times greater during the wet season than during the dry season. Still, in both seasons, the maximum daily TSS could be more than 20 times greater than the average daily

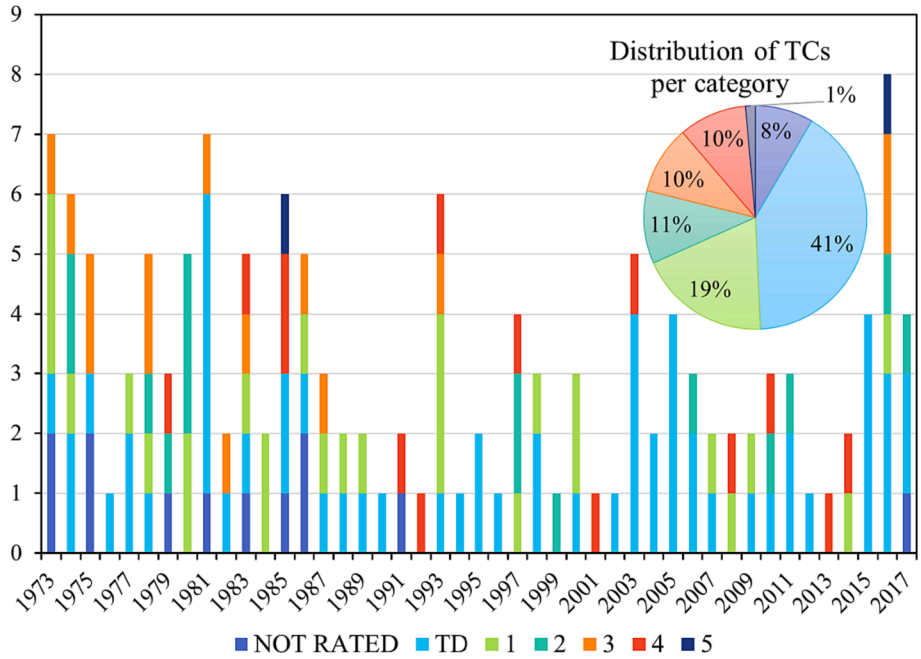

Fig. 9. Number of TCs per season and category from 1972–1973 to 2016 – 2017.

Table 5
Mann-Whitney *U* test p-values comparing the precipitation per TC according to its categories. Bold values denote results that are not statistically significant at the 99% level; the rest are not statistically significant at the 95% level.

	NOT RATED	TD	1	2	3	4
NOT RATED	–	0.433	0.289	0.197	0.313	0.313
TD	0.433	–	**0.023**	**0.014**	0.082	0.055
1	0.289	**0.023**	–	0.757	0.920	0.992
2	0.197	**0.014**	0.757	–	0.503	0.569
3	0.313	0.082	0.920	0.503	–	0.912
4	0.313	0.055	0.992	0.569	0.912	–

value, highlighting the pulsating behaviour of the sediment export. A similar analysis was performed over the daily sediment export. Fig. 7b presents the monthly minimum, maximum and average daily values. Note that from July to November, the minimum value was zero, which means days with no sediment export from the catchment. However, for representation purposes, those values were drawn as lower than 0.000001 tons in the chart. The results showed a similar trend to the TSS, but with higher differences between the average, minimum and maximum daily values. It is important to point out that the sediment exported from the catchment ends up in the reef lagoon and can be recirculated by the tide into the mangrove wetland.

3.3. TCs sediment analysis

During the studied period, 142 TCs were identified within the area of interest (Fig. 8 and Fig. 9), an average of more than three cyclones per year. The Australian Bureau of Meteorology categorised them into five categories according to the maximum mean wind and the typical strongest gust. Only 1 % of the total were category 5 (strongest), 8 % were not rated, 41 % were categorised as a tropical depression (TD), 19 % as category 1, and the rest were evenly divided among categories 2, 3 and 4. The average duration of the cyclones in the area was 3.2 days, with a maximum of 11 days.

The average areal precipitation per event was 100 mm. Nevertheless, it was highly variable and unrelated to the cyclone category (Fig. S.7). Table 5 presents the results of the Mann-Whitney *U* test showing that for the Dreketi catchment, the total average areal precipitation is independent of the cyclone category. Note that TC category five was not included in the analysis because the number of events was insufficient.

The relative contribution of the TCs to the total annual precipitation (areal average) is shown in Fig. 10 (blue bars). On average, 13.7 % of the annual precipitation is related to a TC. However, it varies from year to year (1 % up to 37 %) and can be linked to the number of cyclones per season. The green bars in Fig. 10 represent the average contribution per TC to the annual precipitation, showing an average contribution of 5 %. Analysing the maximum daily values, it was found that the maximum daily precipitation was related to a TC in 15 out of 45 years.

Using the calibrated model, the impact of TCs was assessed. On average, the overall contribution of TCs to the annual sediment export was 23.5 % (Fig. 10b); however, this varies from as low as 1.4 % to as high as 80.4 %). This contribution of TCs to sediment expert is higher than the contribution of TCs to total precipitation (13.7 %). The higher contribution of TCs to the total annual sediment export than to the annual precipitation can be explained by analysing the relation between precipitation and sediment export for each event (Fig. 11). It was observed that the same amount of precipitation could generate more than three times more sediment if the event can be related to TCs, due to the higher precipitation intensity. Table 6 compares the average and maximum daily intensity and total precipitation for TC-related and unrelated events. The average daily intensity is 2.7 times greater for TCs, and the maximum intensity per event is up to three times greater. These differences are more noticeable when the sediment export is analysed. On average, the amount of sediment exported per TC was 8480 tons per event, six times greater than was generated by other storms (1350 tons per event). A nonparametric analysis of the sediment export produced by TCs and nonTCs events was performed. The Mann-Whitney *U* test showed that there is a significant difference between the two classifications with a confidence level of 95 % ($p = 0.000$), similar results were found for the comparison of total precipitation and intensity.

Analysing the extreme values of sediment export, we found that in 35.6 % of the cases the maximum annual value was due to a TC. The average of those maximum sediment export values represents 21.8 % of the annul total annual, with extreme cases such as cyclone RAJA in the season of 1986–1987 that produced 67 % of the annual sediment export in one day.

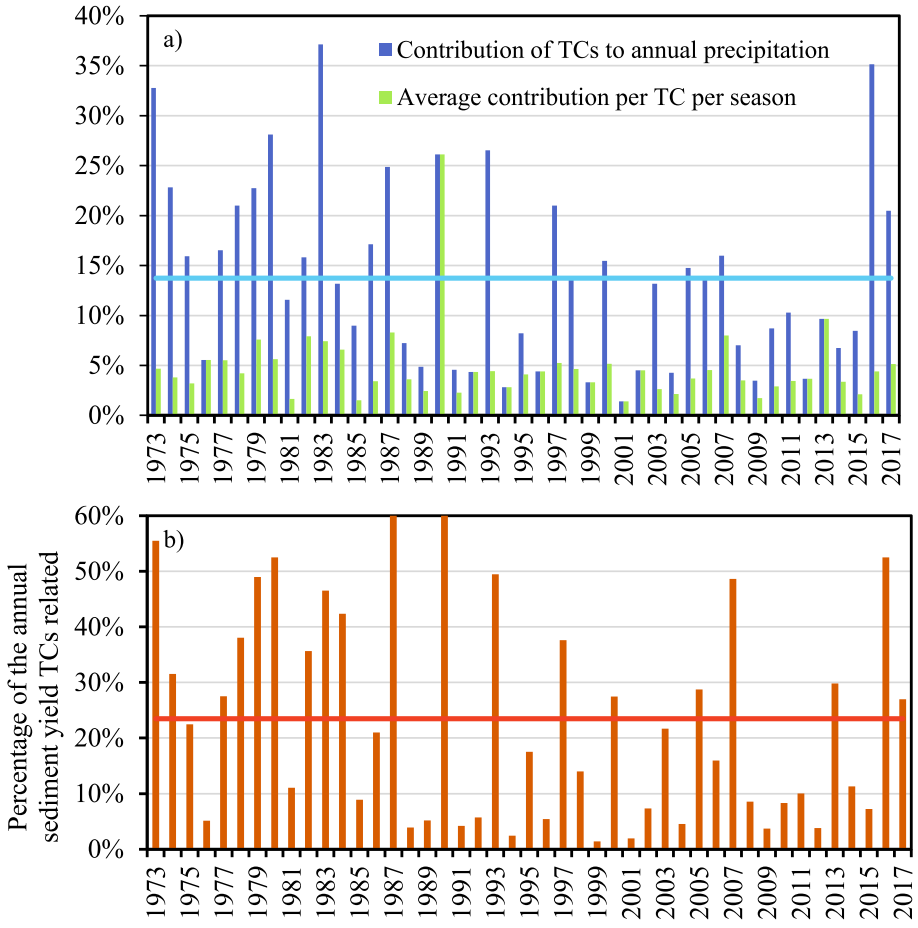

Fig. 10. a) Contribution of TCs to the annual precipitation per year and per cyclone. b) Contribution of TCS to the annual sediment export.

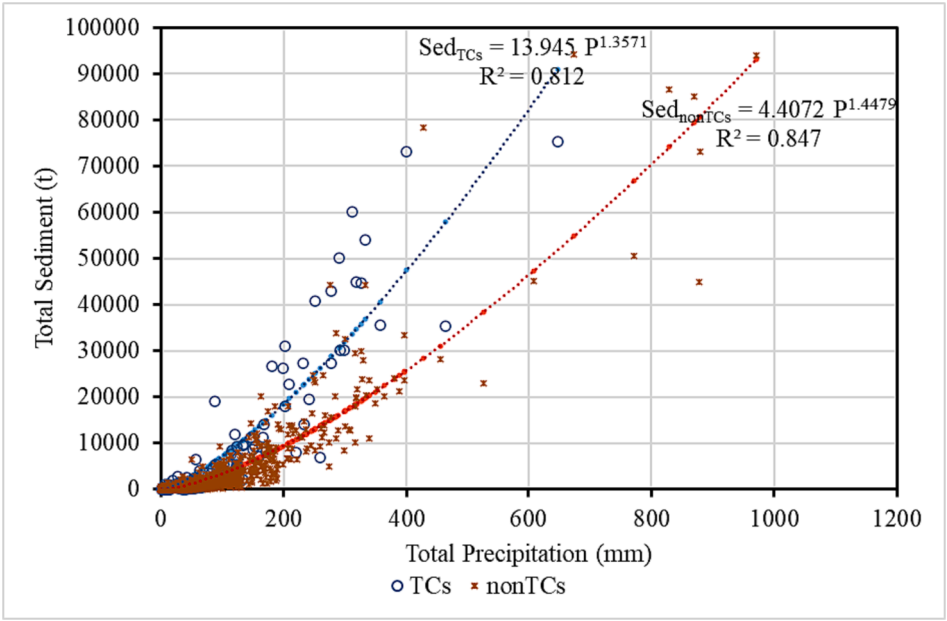

Fig. 11. Total sediment export versus total precipitation per event classified according to their origin.

4. Discussion

The objectives of this work were to characterise the hydro-sedimentological behaviour of the catchment; and to assess the impact of TCs on the annual sediment export and explore the relationship between precipitation and sediment export for TC-related and TC-unrelated events.

Table 6
Average features of TCs and nonTCs events.

	Intensity (mm/day)		Total Precipitation (mm)
	Average	Maximum	
TCs	25.0	54.8	104.4
nonTCs	9.2	18.2	38.1

4.1. Hydro-sedimentological modelling of the catchment

The simulation results showed the ability of the model to capture the response of the Dreketi River catchment, regardless of the limited availability of input data and the complexity of the catchment. The simulated runoff was able to represent the bankfull discharge at the Natua pump station. The peaks could not be reproduced because the model simulates with a daily time step, while the process at that sub-catchment occur at sub-daily scale considering the topography (average slope 20 %) and the area of the sub-catchment (128 km^2). Fig. 12 presents the results at the catchment outlet for the wet season 1989 – 1990. The average daily flow generated by cyclone RAJA stands out as the maximum value of the year, agreeing with the bibliography that acknowledges it as one of the worst flooding events in Vanua Levu island (McGree et al., 2010, Terry and Raj, 1999b).

Regarding the sediment export at the catchment outlet, the range of values is comparable with estimates from Brown et al. (2017), who obtained, on average per wet season 63,000 ton/year (2003 – 2011). Our estimate for the same period was slightly higher at 89,000 ton/year. However, the differences could be explained by the land cover data input. In this study, five types of land cover were considered, while previous studies worked with two types of land cover, forested and not forested, combing in the last one urban and rural areas.

The model allowed us to assess the sediment connectivity of the catchment (Saco et al., 2020) and the relation between the areas of sediment production, deposition, and transport. The sediment yield within the catchment was higher in the headwater sub-catchments, but the sediment export was limited by the transport capacity of the lower plain streams. When those rivers reached their maximum capacity, a substantial proportion of sediment was deposited. The accretion rate for the lower plain sub-catchments was calculated using the annual average deposition, the area of the floodplain and the specific weight of the soil, resulting in a value of 25 mm/year. This value agrees with measurements from Terry et al. (2008), who conducted a study based on ^{137}Cs on the lower plain of the Labasa River (adjacent to the Dreketi River) and found a rate of accretion of 27 mm/year +- 2 mm.

4.2. TCs sediment analysis

The comparison of the total precipitation of TCs and nonTCs showed that for the average areal precipitation of the catchment, there is no link between the precipitation and the category of the cyclones. This particular characteristic of the tropical cyclones in Fiji has been observed by Terry (2007), who described all factors affecting the precipitation during a tropical cyclone. More recently, Sharma et al. (2021) arrived at similar conclusions for extreme precipitation events in three Fijian meteorological stations when analysing the daily precipitation data.

The average contribution of TCs to the annual precipitation is 13.7 % and generates on average, 23.5 % of the annual sediment export, according to the results from the hydro-sedimentological model. A link with precipitation intensity was identified, indicating that the TC-related events are 2.7 times more intense on average than nonTC events. This higher intensity produces more than three times more sediment export, for the same total precipitation. Analysis of sediment export per event showed that TC-related events produced on average more than six times the sediment export of nonTC events.

Finally, the analysis of maximum daily values revealed that in 33.3 % of cases, the maximum daily precipitation was TC-related. Similar values were reported for the area (Deo et al., 2021). Furthermore, 35.6 % of the maximum daily sediment export is TC-related contributing on average with 21.8 % of the annual sediment export in a single day.

5. Conclusions

Access to reliable information is a major challenge in many developing countries, including Pacific Island countries. By using remote sensing data and limited on-ground data, we were able to calibrate the sedimentological model and obtain insights into the hydro-sedimentological behavior of the Dreketi River catchment. A main feature identified was the strong contribution of the headwaters to the annual sediment yield, although the transport capacity of the lower plain sub-catchments limited the sediment export. Another important

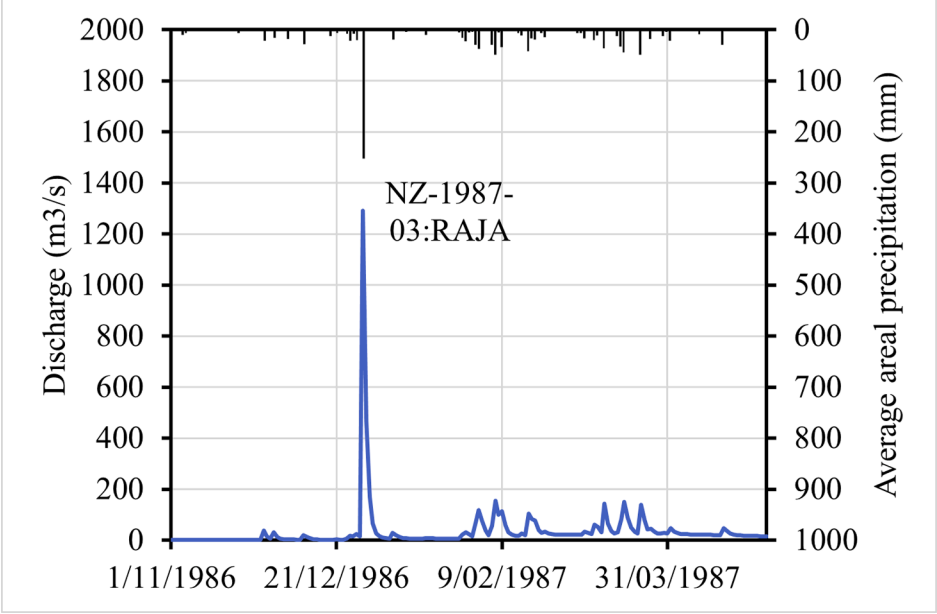

Fig. 12. Daily precipitation and discharge from the Dreketi River catchment during the wet season 1986 – 1987.

finding was the strong relationship between sediment export and tropical cyclones, which is explained by the higher precipitation intensity of these events. The analysis of the data showed that TC-related events were, on average, three times more intense in terms of precipitation rate. Those events could export up to six times more sediment than non TC-related events. Our results highlight the critical link between precipitation rate and sediment export, particularly given the predicted increase in higher precipitation intensities due to a warmer world (IPCC, 2021). This knowledge is vital for assessing erosion risks, managing water quality, planning resilient infrastructure, guiding climate change adaptation strategies, protecting ecosystems, and informing policy decisions. It can help decision-makers in land use planning, watershed management, and ecosystem restoration to consider the potential impacts of sediment export in a changing climate and take action accordingly.

CRediT authorship contribution statement

Eliana Jorquera: Conceptualization, Methodology, Software, Investigation, Visualization, Formal analysis, Writing – original draft. **Patricia M. Saco:** Conceptualization, Supervision, Formal analysis, Writing – review & editing, Funding acquisition. **Danielle Verdon-Kidd:** Supervision, Formal analysis, Writing – review & editing. **José F. Rodríguez:** Conceptualization, Supervision, Formal analysis, Writing – review & editing. **Herman Timmermans:** Writing – review & editing. **Filomena Nelson:** Writing – review & editing.

Declaration of competing interest

The authors declare that they have no known competing financial interests or personal relationships that could have appeared to influence the work reported in this paper.

Data availability

Data will be made available on request.

Acknowledgements

This research was funded by the University of Newcastle Postgraduate Research Scholarship (UNRSC) (E.J.). Additional funding was provided by the Australian Research Council through grant FT140100610 (P.M.S.). We are grateful to the Fiji Meteorological Service for providing the meteorological data.

Appendix A. Supplementary material

Supplementary data to this article can be found online at https://doi.org/10.1016/j.catena.2024.107805.

References

Abdelwahab, O.M.M., Ricci, G.F., de Girolamo, A.M., Gentile, F., 2018. Modelling soil erosion in a Mediterranean watershed: Comparison between SWAT and AnnAGNPS models. Environ. Res. 166, 363–376.

Agrawala, S., Ota, T., Risbey, J., Hagenstad, M., Smith, J., Van Aalst, M., Koshy, K., Prasad, B., 2003. Development and Climate Change in Fiji: Focus on coastal mangroves. OECD.

Alvarez-Romero, J.G., Wilkinson, S.N., Pressey, R.L., Ban, N.C., Kool, J., Brodie, J., 2014. Modeling catchment nutrients and sediment loads to inform regional management of water quality in coastal-marine ecosystems: a comparison of two approaches. J. Environ. Manage. 146, 164–178.

Arnold, J.G., Srinivasan, R., Muttiah, R.S., Williams, J.R., 1998. Large area hydrologic modeling and assessment part I: Model Development. JAWRA J. Am. Water Resour. Assoc. 34, 73–89.

Barnes, P., 2020. A Pacific disaster prevention review. Australian Strategic Policy Institute.

Behlert, B., Diekjobst, R., Felgentreff, C., Manandhar, T., Mucke, P., Pries, L., Radtke, K., Weller, D., 2020. WorldRiskReport 2020. The WorldRiskIndex, Bündnis Entwicklung Hilf.

Benavidez, R., Jackson, B., Maxwell, D., Norton, K., 2018. A review of the (Revised) Universal Soil Loss Equation (R/USLE): with a view to increasing its global applicability and improving soil loss estimates. Hydrol. Earth Syst. Sci. Discuss. 1–34.

Bingner, R., Theurer, F., 2001. AGNPS 98: A Suite of Water Quality Models For Watershed Use. Federal Interagency Sedimentation Conference Proceedings, 2001 Reno, Nevada.

Bingner, R., Theurer, F., 2016. AGNPS Web Site [Online]. Available: http://www.ars.usda.gov/Research/docs.htm?docid=5199 [Accessed].

Breda, A., Saco, P.M., Sandi, S.G., Saintilan, N., Riccardi, G., Rodríguez, J.F., 2021. Accretion, retreat and transgression of coastal wetlands experiencing sea-level rise. Hydrol. Earth Syst. Sci. 25, 769–786.

Breda, A., Saco, P.M., Rodríguez, J.F., Sandi, S.G., Riccardi, G., 2022. Assessing the effects of sediment and tidal level variability on coastal wetland evolution. J. Hydrol. 613, 128387.

Briak, H., Moussadek, R., Aboumaria, K., Mrabet, R., 2016. Assessing sediment yield in Kalaya gauged watershed (Northern Morocco) using GIS and SWAT model. Int. Soil Water Conserv. Res. 4, 177–185.

Brockmann, C., Doerffer, R., Peters, M., Kerstin, S., Embacher, S., Ruescas, A., 2016. Evolution of the C2RCC neural network for Sentinel 2 and 3 for the retrieval of ocean colour products in normal and extreme optically complex waters. Living Planet Symposium 54.

Brown, C.J., Jupiter, S.D., Albert, S., Klein, C.J., Mangubhai, S., Maina, J.M., Mumby, P., Olley, J., Stewart-Koster, B., Tulloch, V., Wenger, A., 2017. Tracing the influence of land-use change on water quality and coral reefs using a Bayesian model. Sci Rep 7, 4740.

Chiu, Y.-J., Lee, H.-Y., Wang, T.-L., Yu, J., Lin, Y.-T., Yuan, Y., 2019. Modeling Sediment Yields and Stream Stability Due to Sediment-Related Disaster in Shihmen Reservoir Watershed in Taiwan. Water 11, 332.

Dare, R.A., Davidson, N.E., McBride, J.L., 2012. Tropical Cyclone Contribution to Rainfall over Australia. Mon. Weather Rev. 140, 3606–3619.

de Vente, J., Poesen, J., Verstraeten, G., Govers, G., Vanmaercke, M., van Rompaey, A., Arabkhedri, M., Boix-Fayos, C., 2013. Predicting soil erosion and sediment yield at regional scales: Where do we stand? Earth Sci. Rev. 127, 16–29.

Deo, A., Chand, S.S., Ramsay, H., Holbrook, N.J., McGree, S., Magee, A., Bell, S., Titimaea, M., Haruhiru, A., Malsale, P., Mulitalo, S., Daphne, A., Prakash, B., Vainikolo, V., Koshiba, S., 2021. Tropical cyclone contribution to extreme rainfall over southwest Pacific Island nations. Clim. Dyn.

Diamond, H.J., Lorrey, A.M., Knapp, K.R., Levinson, D.H., 2012. Development of an enhanced tropical cyclone tracks database for the southwest Pacific from 1840 to 2010. Int. J. Climatol. 32, 2240–2250.

Doerffer, R., Schiller, H., 2007. The MERIS Case 2 water algorithm. Int. J. Remote Sens. 28, 517–535.

Eslinger, D.L.H., Carter, J., Pendleton, M., Burkhalter, S., Allen, M., 2014. Technical Guide for OpenNSPECT - Version 1.2. National Oceanic and Atmospheric Administration (NOAA) Coastal Services Center.

Fernandez, O.V.Q., 2017. Bankfull hydraulic geometry relationships for rivers and streams of the western and southwest regions of Paraná State, Brazil. J. Geogr. 5, 50-63.

Fiji Meteorological Service, 2006. The Climate of Fiji.

García, C.M., Caamaño Nelli, G.E., Dasso, C.M., 2001. Estimación de láminas máximas de lluvia a partir de información pluviométrica diaria.

Gordon, N.D., McMahon, T.A., Finlayson, B.L., Gippel, C.J., Nathan, R.J., 2004. Stream hydrology: an introduction for ecologists. John Wiley and Sons.

Government of Fiji, 2017. Climate vulnerability assessment: Making Fiji climate resilient, World Bank.

Hajigholizadeh, M., Melesse, A.M., Fuentes, H.R., 2018. Erosion and Sediment Transport Modelling in Shallow Waters: A Review on Approaches, Models and Applications. Int. J. Environ. Res. Public Health 15, 518.

Harrelson, C.C., Rawlins, C.L., Potyondy, J.P., 1994. Stream channel reference sites: an illustrated guide to field technique. General Technical Report RM-245. Fort Collins, CO: US Department of Agriculture, Forest Service, Rocky Mountain Forest and Range Experiment Station.

Hudson, N., 1993. Field measurement of soil erosion and runoff, Food & Agriculture Org.

Intergovernmental Panel on Climate Change, 2021. Climate Change 2021: The Physical Science Basis. Contribution of Working Group I to the Sixth Assessment Report of the Intergovernmental Panel on Climate Change, Cambridge, United Kingdom and New York, NY, USA, Cambridge University Press.

International Union of Soil Sciences Working Group WRB, 2022. World Reference Base for Soil Resources. International soil classification system for naming soils and creating legends for soil maps. 4th edition., Vienna, Austria.

Iqbal, M., 1983. An Introduction to Solar Radiation, Canada, Academic Press.

Jorquera, E., Rodríguez, J.F., Saco, P.M., Timmermans, H., 2019. Assessment of the impact of cyclones on the annual sediment budget in a Pacific Island catchment using a hydro-sedimentological model. In: Elsawah, S., ed. MODSIM2019, 23rd International Congress on Modelling and Simulation., 2019 Canberra, Australia. Modelling and Simulation Society of Australia and New Zealand, 972-978.

Khouakhi, A., Villarini, G., Vecchi, G.A., 2017. Contribution of Tropical Cyclones to Rainfall at the Global Scale. J. Clim. 30, 359–372.

Knisel, W.G., Douglas-Mankin, K.R., 2012. CREAMS/GLEAMS: Model Use, Calibration, and Validation. Trans. ASABE 55, 1291–1302.

Knisel, W.G., 1980. CREAMS: A field scale model for chemicals, runoff, and erosion from agricultural management systems, Department of Agriculture, Science and Education Administration.

Kostaschuk, R.A.Y., Terry, J., Raj, R., 2001. Tropical cyclones and floods in Fiji. Hydrol. Sci. J. 46, 435–450.

Lafale, P.F., Diamond, H.J., Anderson, C.L., 2018. Effects of Climate Change on Extreme Events Relevant to the Pacific Islands. Science Review 2018. Pacific Marine Climate Change Report Card.
Li, L., Wang, Y., Liu, C., 2014. Effects of land use changes on soil erosion in a fast developing area. Int. J. Environ. Sci. Technol. 11, 1549–1562.
Liu, Y., Li, S., Wallace, C.W., Chaubey, I., Flanagan, D.C., Theller, L.O., Engel, B.A., 2017. Comparison of Computer Models for Estimating Hydrology and Water Quality in an Agricultural Watershed. Water Resour. Manag. 31, 3641–3665.
Magee, A.D., Verdon-Kidd, D.C., Kiem, A.S., 2016a. An intercomparison of tropical cyclone best-track products for the southwest Pacific. Nat. Hazards Earth Syst. Sci. 16, 1431–1447.
Magee, A.D., Verdon-Kidd, D.C., Kiem, A.S., Royle, S.A., 2016b. Tropical cyclone perceptions, impacts and adaptation in the Southwest Pacific: an urban perspective from Fiji, Vanuatu and Tonga. Nat. Hazards Earth Syst. Sci. 16, 1091–1105.
Mangubhai, S., Sykes, H., Lovell, E., Brodie, G., Jupiter, S., Morris, C., Lee, S., Loganimoce, E. M., Rashni, B., Lal, R., Nand, Y., Qauqau, I., 2019. Chapter 35 - Fiji: Coastal and Marine Ecosystems. In: Sheppard, C. (ed.) World Seas: an Environmental Evaluation (Second Edition). Academic Press.
McGree, S., Yeo, S.W., Devi, S., 2010. Flooding in the Fiji Islands between 1840 and 2009. Risk Frontiers.
McInnes, K.L., Walsh, K.J.E., Hoeke, R.K., O'Grady, J.G., Colberg, F., Hubbert, G.D., 2014. Quantifying storm tide risk in Fiji due to climate variability and change. Global Planet. Change 116, 115–129.
Merritt, W.S., Letcher, R.A., Jakeman, A.J., 2003. A review of erosion and sediment transport models. Environ. Model. Softw. 18, 761–799.
Moriasi, D.N., Arnold, J.G., van Liew, M.W., Bingner, R.L., Harmel, R.D., Veith, T.L., 2007. Model evaluation guidelines for systematic quantification of accuracy in watershed simulations. Trans. ASABE 50, 885–900.
Nazirova, K., Alferyeva, Y., Lavrova, O., Shur, Y., Soloviev, D., Bocharova, T., Strochkov, A., 2021. Comparison of In Situ and Remote-Sensing Methods to Determine Turbidity and Concentration of Suspended Matter in the Estuary Zone of the Mzymta River, Black Sea. Remote Sens. 13, 143.
Neitsch, S.L., Arnold, J.G., Kiniry, J.R., Williams, J.R., 2011. Soil and Water Assessment Tool Theoretical Documentation Version 2009. Texas Water Resources Institute Technical Report No 406. College Station, Texas.: Texas A&M University System.
Nguyen, H.H., Recknagel, F., Meyer, W., Frizenschaf, J., Ying, H., Gibbs, M.S., 2019. Comparison of the alternative models SOURCE and SWAT for predicting catchment streamflow, sediment and nutrient loads under the effect of land use changes. Sci. Total Environ. 662, 254–265.
Notebaert, B., Vaes, B., Verstraeten, G., Govers G., van Oost, K., van Rompaey, A., 2006. WaTEM-SEDEM version 2006 Manual. Physical and Regional Geography Research Group.
Pacific Catastrophe Risk Assessment and Financing Initiative, 2010. Republic of Fiji - Landuse Landcover Map.
Pandey, A., Himanshu, S.K., Mishra, S., Singh, V.P., 2016. Physically based soil erosion and sediment yield models revisited. Catena 147, 595–620.
Quijano-Baron, J., Saco, P.M., Rodriguez, J.F., 2022. Modelling the effects of above and belowground biomass pools on erosion dynamics. Catena 213, 106123.
Ramsar Convention Secretariat, 2019. The list of wetlands of international importance. RAMSAR Secretariat: Gland, Switzerland.
Ricci, G.F., de Girolamo, A.M., Abdelwahab, O.M.M., Gentile, F., 2018. Identifying sediment source areas in a Mediterranean watershed using the SWAT model. Land Degrad. Dev. 29, 1233–1248.
Rodriguez, J.F., Saco, P.M., Sandi, S., Saintilan, N., Riccardi, G., 2017. Potential increase in coastal wetland vulnerability to sea-level rise suggested by considering hydrodynamic attenuation effects. Nat Commun 8, 16094.
Saco, P.M., McDonough, K.R., Rodriguez, J.F., Rivera-Zayas, J., Sandi, S.G., 2021. The role of soils in the regulation of hazards and extreme events. Philos. Trans. R. Soc., B 376, 20200178.
Sandi, S.G., Rodríguez, J.F., Saintilan, N., Riccardi, G., Saco, P.M., 2018. Rising tides, rising gates: The complex ecogeomorphic response of coastal wetlands to sea-level rise and human interventions. Adv. Water Resour. 114, 135–148.
Secretariat of the Pacific Regional Environment Programme, 2017. Ecosystem & Socio-economic Resilience Analysis & Mapping (ESRAM) for Macuata Province, Fiji. In: Programme, P.R.E. (ed.) Pacific Ecosystem-Based Adaption to Climate Change Project. www.sprep.org/pebacc.
Sharma, K.K., Verdon-Kidd, D.C., Magee, A.D., 2020. Decadal variability of tropical cyclogenesis and decay in the southwest Pacific. Int. J. Climatol. 40, 2811–2829.
Sharma, K.K., Verdon-Kidd, D.C., Magee, A.D., 2021. A decision tree approach to identify predictors of extreme rainfall events – A case study for the Fiji Islands. Weather Clim. Extremes 34, 100405.
Sharp, R., Chaplin-Kramer, R., Wood, S., Guerry, A., Tallis, H., Ricketts, T., Nelson, E., Ennaanay, D., Wolny, S., Olwero, N., Vigerstol, K., Pennington, D., Mendoza, G., Aukema, J., Foster, J., Forrest, J., Cameron, D., Arkema, K., Lonsdorf, E., Kennedy, C., Verutes, G., Kim, C.-K., Guannel, G., Papenfus, M., Toft, J., Marsik, M., Bernhardt, J., Griffin, R., Glowinski, K., Chaumont, N., Perelman, A., Lacayo, M., Mandle, L., Hamel, P., Vogl, A.L., Rogers, L., Bierbower, W., Denu, D., Douglass, J., 2018. InVEST User's Guide. The Natural Capital Project, Stanford University, University of Minnesota, The Nature Conservancy, and World Wildlife Fundation.
Smith, D.D., Wischmeier, W.H., 1957. Factors affecting sheet and rill erosion. Eos Trans. AGU 38, 889–896.
Terry, J.P., Raj, R., 1999a. The 1997–98 El Niño and drought in the Fiji Islands. Hydrology and water management in the humid tropics. Proceedings of the second international colloquium, 22-26.
Terry, J.P., Raj, R., 1999b. Island environment and landscape responses to 1997 tropical cyclones in Fiji.
Terry, J.P., Gienko, G., 2010. Climatological aspects of South Pacific tropical cyclones, based on analysis of the RSMC-Nadi (Fiji) regional archive. Climate Res. 42, 223–233.
Terry, J.P., McGree, S., Raj, R., 2004. The Exceptional Flooding on Vanua Levu Island, Fiji, during Tropical Cyclone Ami in January 2003. J. Nat. Dis. Sci. 26, 27–36.
Terry, J.P., Lal, R., Garimella, S., 2008. An Examination of Vertical Accretion of Floodplain Sediments in the Labasa River Sugarcane Belt of Northern Fiji: Rates, Influences and Contributing Processes. Geogr. Res. 46, 399–412.
Terry, J.P., 2007. Tropical cyclones: climatology and impacts in the South Pacific. Springer Science & Business Media.
TUCCI, 2012. Hidrologia: ciência e aplicação.
Vigerstol, K.L., Aukema, J.E., 2011. A comparison of tools for modeling freshwater ecosystem services. J Environ Manage 92, 2403–2409.
Vilaysane, B., Takara, K., Luo, P., Akkharath, I., Duan, W., 2015. Hydrological Stream Flow Modelling for Calibration and Uncertainty Analysis Using SWAT Model in the Xedone River Basin, Lao PDR. Procedia Environ. Sci. 28, 380–390.
Villarini, G., Denniston, R.F., 2016. Contribution of tropical cyclones to extreme rainfall in Australia. Int. J. Climatol. 36, 1019–1025.
Wilkinson, S.N., Prosser, I.P., Rustomji, P., Read, A.M., 2009. Modelling and testing spatially distributed sediment budgets to relate erosion processes to sediment yields. Environ. Model. Softw. 24, 489–501.
Williams, J.R., Berndt, H.D., 1977. Sediment Yield Prediction Based on Watershed Hydrology. Trans. ASAE 20, 1100–1104.
Wischmeier, W.H., Smith, D.D., Uhland, R., 1958. Evaluation of factors in the soil loss equation. Agri. Eng. 39, 458–462.
Wischmeier, W.H., 1959. A Rainfall Erosion Index for a Universal Soil-Loss Equation1. Soil Sci. Soc. Am. J. 23, 246-249.
Wolman, M.G., Leopold, L.B., 1957. River flood plains: Some observations on their formation. Professional Paper, Washington, D.C.
World bank group, 2017. Pacific Possible : long-term economic opportunities and challenges for Pacific Island Countries (English). Pacific Possible Series, Washington, D.C.
Wu, C.-H., Chen, C.-N., Tsai, C.-H., Tsai, C.-T., 2012. Estimating sediment deposition volume in a reservoir using the physiographic soil erosion-deposition model. Int. J. Sedim. Res. 27, 362–377.
Yáñez-Arancibia, A., Day, J.W., Knoppers, B.A., Jiménez, J.A., 2011. Coastal Lagoons and Estuaries.

Further reading

The EBM Approach. In: Fanning, L., Mahon, R., Mcconney, P. (eds.) Towards Marine Ecosystem-Based Management in the Wider Caribbean. Amsterdam University Press.